

Abstract

The regional climate model MAR including a coupled snow pack/aeolian snow transport parameterisation is compared with aeolian snow mass fluxes at a fine spatial resolution (5 km horizontally and 2 m vertically) and at a fine temporal resolution (30 min) over 1 month in Antarctica. Numerous feedbacks are taken into account in the MAR including the drag partitioning caused by the roughness elements. Wind speed is correctly simulated with a positive value of the Nash test (0.60 and 0.37) but the wind speeds above 10 m s^{-1} are underestimated. The aeolian snow transport events are correctly reproduced with a good temporal resolution except for the aeolian snow transport events with a particles' maximum height below 1 m. The simulated threshold friction velocity, calculated without snowfall, is overestimated. The simulated aeolian snow mass fluxes between 0 to 2 m have the same variations but are underestimated compared to the second-generation FlowCapt values and so is the simulated relative humidity at 2 m. This underestimation is not entirely due to the underestimation of the simulated wind speed. The MAR underestimates the aeolian snow quantity that pass through the first two meters by a factor ten compared to the second-generation FlowCapt value (13990 kg m^{-1} and 151509 kg m^{-1} respectively). It will conduct the MAR, with this parametrisation, to underestimate the effect of the aeolian snow transport on the Antarctic surface mass balance.

1 Introduction

Aeolian snow mass flux measurements in Antarctica reveal that a large amount of snow is transported by the wind (Budd, 1966; Mann et al., 2000; Trouvilliez et al., 2014; Wendler, 1989). The aeolian snow transport and its subsequent sublimation is probably a significant component of the surface mass balance of the Antarctic ice sheet (ASMB). Previous estimations of the contribution of aeolian snow transport to the ASMB using numerical models were reported to be around 10% (Déry and Yau, 2002; Lenaerts

Comparison of aeolian snow transport events and snow mass fluxes

A. Trouvilliez et al.

Title Page

Abstract

Introduction

Conclusions

References

Tables

Figures

◀

▶

◀

▶

Back

Close

Full Screen / Esc

Printer-friendly Version

Interactive Discussion



by Bintanja (2000). The sublimation of the blown particle is computed by the microphysical scheme and has an effect on the heat and moisture budgets in the layer where the sublimation occurs. Aeolian snow transport also has an effect on the radiative transfer through the atmosphere as it can change the atmospheric optical depth (Gallée and Gorodetskaya, 2010). Densification of the snowpack by the wind is included from the work of Kotlyakov (1961), i.e. the snow density increases with an increase in the wind speed and thus the threshold friction velocity will be higher.

The threshold friction velocity for a smooth surface depends on the snowpack characteristics: the dendricity, the sphericity and the grain size for density below 330 kg m^{-3} as in Guyomarc'h and Mérindol (1998), and the snow density above 330 kg m^{-3} . To account for the drag partition caused by the roughness elements, the threshold friction velocity for a rough surface is calculated as in Marticorena and Bergametti (1995):

$$u_{*tR} = \frac{u_{*tS}}{R_f} \quad (1)$$

Where u_{*tR} is the threshold friction velocity for a rough surface, u_{*tS} is the threshold friction velocity for a smooth surface and R_f is a ratio factor defined as:

$$R_f = 1 - \left[\frac{\ln\left(\frac{z_{0R}}{z_{0S}}\right)}{\ln\left(0.35\left(\frac{10}{z_{0S}}\right)^{0.8}\right)} \right] \quad (2)$$

where z_{0R} and z_{0S} are the surface roughness lengths for rough and smooth surfaces, respectively, in meters. The sensitivity of R_f to z_{0S} is small for a value of z_{0S} above $5 \times 10^{-5} \text{ m}$ (Marticorena and Bergametti, 1995). The general value of the roughness height of smooth snow cover is around 10^{-5} – 10^{-4} m (Leonard et al., 2011). In addition to the drag partition, moving particles in the saltation layer transfer momentum from the airflow to the surface. Above the saltation layer, the net effect is similar to

Comparison of
aeolian snow
transport events and
snow mass fluxes

A. Trouvilliez et al.

Title Page

Abstract

Introduction

Conclusions

References

Tables

Figures

◀

▶

◀

▶

Back

Close

Full Screen / Esc

Printer-friendly Version

Interactive Discussion



that of a stationary roughness element (Owen, 1964). Thus, saltation leads to an increase of the roughness length compared with the roughness length without transport even for a smooth surface. The z_{0S} is determined by a calibration with Byrd project measurements (Budd et al., 1966; Gallée et al., 2001):

$$z_{0S} = 5 \cdot 10^{-5} + \max \left(0.5 \cdot 10^{-6}, 0.536 \cdot 10^{-3} \cdot u_*^2 - 61.8 \cdot 10^{-6} \right) \quad (3)$$

One of the main roughness elements in the Antarctica snowpack is the sastrugi. They are profiled with the main wind direction, and a variation in the wind direction results in a change of the sastrugi drag coefficient and leads to an increase of the roughness height z_{0R} (Jackson and Carroll, 1978). Furthermore, the sastrugi adapt their profile to the new mean direction with a decrease of the coefficient drag to a limit value. Andreas (1995) estimates this time-response to be around half a day. Sastrugi can be buried if precipitation occurs. All these effects are taken into account in the improved version of the snowpack sub-model with the parameterization of the z_{0R} (Gallée et al., 2013), which is a negative feedback on the transport.

Once aeolian transport is initiated, the snow particles' concentration in the saltation layer, in kilograms of particle per kilograms of air, η_S , is parameterized from (Pomeroy, 1989):

$$\eta_S = \begin{cases} 0 & \text{if } u_{*R} < u_{*tR} \\ e_{\text{salt}} \left(\frac{u_{*R}^2 - u_{*tR}^2}{g \cdot h_{\text{salt}}} \right) & \text{if } u_{*R} \geq u_{*tR} \end{cases} \quad (4)$$

where u_{*R} is the friction velocity for a rough surface in ms^{-1} , e_{salt} is the saltation efficiency equal to 3.25, g is the gravitational acceleration in ms^{-2} and h_{salt} is the saltation height in m, a function of u_{*R} (Pomeroy and Male, 1992).

**Comparison of
aeolian snow
transport events and
snow mass fluxes**

A. Trouvilliez et al.

Title Page

Abstract

Introduction

Conclusions

References

Tables

Figures

◀

▶

◀

▶

Back

Close

Full Screen / Esc

Printer-friendly Version

Interactive Discussion



4 Comparison of field data and model

The aim of this section is to provide a detailed comparison between the observed and the modelled meteorological variables including relative humidity and aeolian snow mass fluxes. Modelling results are from a MAR simulation in Adélie Land during January 2011. A spin-up step, as described in Gallée et al. (2013), was applied for current modelling. The modelling grid and set-up are the same as those of Gallée et al. (2013): the integrative domain is a 450 km × 450 km square with a 5 km horizontal resolution (Fig. 1). Lateral forcing and sea-surface conditions are taken from ERA-Interim. There are 60 vertical levels with a first level at 2 m height and a vertical resolution of 2 m in the lowest 12 levels. The simulation started 1 month before the period of interest, i.e. 1 December 2010, in order to get a relative equilibrium of the snow pack with the atmospheric conditions. The model performances are assessed by the statistical test proposed by Nash and Sutcliffe (1970). An efficiency of 1 means a perfect simulation (RMSE = 0) and a value of 0 or less means that the model is not better than a minimalist model whose output constantly equals the mean value of the modelled variable over the studied time period.

The comparison focuses on the wind speed, as it is the driving force of aeolian transport. The timing of the aeolian snow transport events is then studied with an evaluation of the threshold friction velocity, and finally the aeolian snow mass fluxes are analysed. The relative humidity is also analysed to evaluate the aeolian snow transport sublimation. Indeed, it plays an important role in the ASMB (Lenaerts et al., 2012a) and it is crucial to evaluate numerical models at this point.

Wind speed and relative humidity are compared at a height of 2 m above the surface. Relative humidity with respect to the solid state is calculated from the expression of Goff and Gratch (1946). The observed values of aeolian snow mass fluxes from the FlowCaptTM in contact with the ground are compared with the values of simulated snow mass fluxes in the first layer (0–2 m) to assess the detection of aeolian snow transport events. The mean observed snow mass fluxes from 0 to 2 m are compared with the

Comparison of aeolian snow transport events and snow mass fluxes

A. Trouvilliez et al.

Title Page

Abstract

Introduction

Conclusions

References

Tables

Figures



Back

Close

Full Screen / Esc

Printer-friendly Version

Interactive Discussion



mean simulated snow mass flux from 0 to 2 m. As the lowest layer extends up to 2 m above the surface, the coarse resolution of the model does not allow simulations of the strong decrease of aeolian snow mass fluxes in the first meter, whereas 1-D simulation may do so with an affordable numerical time cost (Xiao et al., 2000). In order to correctly estimate the flux with the first level at 2 m, simulations from a 1-D model, with the same transport parameterization used in the 3-D MAR, were performed with different vertical resolutions. A dimensionless correction factor (A) is determined from these simulations:

$$\mu_{IC} = \mu_{IR} \cdot A = \mu_{IR} \cdot \left[2 + 6 \cdot e^{(1.5 \cdot (2 - 0.4))} \right] \quad (5)$$

where μ_{IC} is the corrected flux for the lowest layer (0–2 m) and μ_{IR} the raw flux from the MAR for the lowest layer, both in $\text{g m}^{-2} \text{s}^{-1}$. This correction is effective only if the MAR simulates aeolian snow transport event.

4.1 Wind speed

Wind speed is correctly simulated (Fig. 3), especially at D17, with an efficiency of 0.60 and 0.37, respectively, for D17 and D47. As already noted by Gallée et al. (2013), variations are correctly represented but wind speeds above 10 ms^{-1} are underestimated. This leads to a constant wind speed underestimation of 2 ms^{-1} at D47. This underestimation may be due to the E- ε turbulent scheme used in MAR. It is based on the small eddies concept and it cannot reproduce the large eddies responsible for the deflection of air parcels flowing higher in the boundary layer. The diagnostic wind gust model of Brasseur and Gallée (2002) is an adequate tool for representing the large eddies associated with high wind speeds and can be associated with the MAR outputs. Although the method simulates the wind gusts, it may be used as a tool with which to evaluate the mechanisms involved in the strong wind speed events. The wind gust amplitude simulated by this method corresponds to the maximum mean wind speed observed during strong wind speed events, which corroborates the hypothesis that the underestimation may come from the turbulent scheme.

Comparison of aeolian snow transport events and snow mass fluxes

A. Trouvilliez et al.

Title Page

Abstract

Introduction

Conclusions

References

Tables

Figures

◀

▶

◀

▶

Back

Close

Full Screen / Esc

Printer-friendly Version

Interactive Discussion



clearly be identified for the observed snow mass flux during events 2, 3 and 4 (Fig. 6). For the first event, a hysteresis in the observed snow mass fluxes with the observed wind speed is recorded. Such a hysteresis effect has already been observed (Gordon et al., 2010). This observed variation may be due to a change in the erodible layers.

Indeed, the snow mass flux–wind speed relationship presents three main behaviours through time (Fig. 4, upper left): the first one is characterised by a snow mass flux increase as the wind speed increases, the second one by a strong flux decrease at a nearly constant wind speed, and the third one by a flux decrease as the wind speed decreases but leading the same wind speed to be associated with higher aeolian snow mass flux than during the beginning of the event. It can be explained by the composition of the snowpack with an erodible surface layer, a harder intermediate layer below it with a higher threshold friction velocity, and a third layer, smoother than those above and thus easily erodible. The field reports do not offer additional information to verify this hypothesis and the MAR did not simulate it.

For the simulated snow mass fluxes, the largest occurred for a wind speed around 13 m s^{-1} , clearly visible in the second and fourth events. Modelled fluxes first increase as modelled wind speed increases before the wind speed reaches a stable value, whereas the modelled fluxes continue to increase. This increase is due to the presence of strong simulated precipitations at that time. Thus, the precipitating particles are added to the previous blown snow particles from the surface and increase the aeolian snow mass flux, whereas the wind speed does not change. When the modelled wind speed decrease, so do the modelled fluxes.

Finally, MAR aeolian snow mass fluxes are twice lower than those provided by the second-generation FlowCaptTM with the same wind speed values except when snowfall occurs. Thus, the underestimation of the simulated aeolian snow mass fluxes is not entirely due to the underestimation of the simulated wind speed. Furthermore, MAR is unable to reproduce the strong aeolian snow transport events with observed snow mass fluxes above $100 \text{ g m}^{-2} \text{ s}^{-1}$.

Comparison of aeolian snow transport events and snow mass fluxes

A. Trouvilliez et al.

Title Page

Abstract

Introduction

Conclusions

References

Tables

Figures

◀

▶

◀

▶

Back

Close

Full Screen / Esc

Printer-friendly Version

Interactive Discussion



Comparison of aeolian snow transport events and snow mass fluxes

A. Trouvilliez et al.

Title Page

Abstract

Introduction

Conclusions

References

Tables

Figures

◀

▶

◀

▶

Back

Close

Full Screen / Esc

Printer-friendly Version

Interactive Discussion



the (Sørensen, 1991) formulation may limit the underestimation in the simulation. Next, the drag partition is parameterized with a qualitative formulation (Gallée et al., 2013) based on the work of Jackson and Carroll (1978). In the case of an overestimation of the roughness height, it will lead to a deficit of shear stress available for snow erosion in the simulation and an overestimation of the threshold friction velocity. Considering Eq. (4), it leads also to an underestimation of the simulated snow mass fluxes. As the form drag is the main contributor to roughness height, a further calibration of the roughness height in the MAR is needed. Finally the densification process in the snowpack is based on the (Kotlyakov, 1961) formulation. An overestimation of the snow density will lead to an underestimation of the aeolian snow mass fluxes. Current observations cannot evaluate the simulated roughness height and snow density in the period of interest.

The comparison presented here is a step forward in the evaluation of the aeolian transport of snow by regional climate models. However, there are still processes to be evaluated and calibrated in the models that may be done with observations in simple atmospheric conditions such as in Antarctica compared with mountainous regions. Therefore, new observations are under way with roughness height and snow surface density measurements in Adélie Land. Furthermore, a comparison using remote sensing techniques, which give information on a large scale, and automatic weather and snow stations, which detect sensible small-magnitude events, will be able to evaluate the models more extensively.

Acknowledgements. This comparison would not have been possible without the financial support of the European program FP-7 ICE2SEA, grant no. 226375, and the financial and logistical support of the French polar institute IPEV (program CALVA-1013). Additional support by INSU through the LEFE/CLAPA project and OSUG through the CENACLAM/GLACIOCLIM observatory is also acknowledged. We would like to thank all the on-site personnel in Dumont D'Urville and Cap Prud'homme for their help. We acknowledge the Idris Computing Center for providing computer time.

Comparison of aeolian snow transport events and snow mass fluxes

A. Trouvilliez et al.

Title Page

Abstract

Introduction

Conclusions

References

Tables

Figures

◀

▶

◀

▶

Back

Close

Full Screen / Esc

Printer-friendly Version

Interactive Discussion



2010) based on regional atmospheric climate modeling, *Geophys. Res. Lett.*, 39, 1–5, doi:10.1029/2011GL050713, 2012a.

Lenaerts, J. T. M., van den Broeke, M. R., Déry, S. J., van Meijgaard, E., van de Berg, W. J., Palm, S. P., and Sanz Rodrigo, J.: Modeling drifting snow in Antarctica with a regional climate model: 1. Methods and model evaluation, *J. Geophys. Res.*, 117, D05108, doi:10.1029/2011JD016145, 2012b.

Lenaerts, J. T. M., Van Den Broeke, M. R., Scarchilli, C., and Agosta, C.: Impact of model resolution on simulated wind, drifting snow and surface mass balance in Terre Adélie, East Antarctica, *J. Glaciol.*, 58, 821–829, doi:10.3189/2012JoG12J020, 2012c.

Leonard, K. C., Tremblay, L.-B., Thom, J. E., and MacAyeal, D. R.: Drifting snow threshold measurements near McMurdo station, Antarctica: a sensor comparison study, *Cold Reg. Sci. Technol.*, 70, 71–80, doi:10.1016/j.coldregions.2011.08.001, 2011.

Lorius, C.: Contribution to the knowledge of the Antarctic ice sheet: a synthesis of glaciological measurements in Terre Adélie, *J. Glaciol.*, 4, 79–92, 1962.

Madigan, C. T.: Meteorology. Tabulated and reduced records of the Cape Denison Station, Adélie Land. Australasian Antarctic Expedition 1911–1914 Scientific Reports, Serie B, Vol. 4., 1929.

Mann, G. W., Anderson, P. S., and Mobbs, S. D.: Profile measurements of blowing snow at Halley, Antarctica, *J. Geophys. Res.*, 105, 24491–24508, doi:10.1029/2000JD900247, 2000.

Marticorena, B. and Bergametti, G.: Modeling the atmospheric dust cycle: 1. Design of a soil-derived dust emission scheme, *J. Geophys. Res.*, 100, 16415–16430, 1995.

Naaim-Bouvet, F., Bellot, H., and Naaim, M.: Back analysis of drifting-snow measurements over an instrumented mountainous site, *Ann. Glaciol.*, 51, 207–217, doi:10.3189/172756410791386661, 2010.

Nash, J. E. and Sutcliffe, J. V.: River flow forecasting through conceptual models Part 1 – A discussion of principles, *J. Hydrol.*, 10, 282–290, 1970.

Owen, P. R.: Saltation of uniform grains in air, *J. Fluid Mech.*, 20, 225–242, 1964.

Palermé, C., Kay, J. E., Genthon, C., L'Ecuyer, T., Wood, N. B., and Claud, C.: How much snow falls on the Antarctic ice sheet?, *The Cryosphere*, 8, 1577–1587, doi:10.5194/tc-8-1577-2014, 2014.

Palm, S. P., Yang, Y., Spinhirne, J. D., and Marshak, A.: Satellite remote sensing of blowing snow properties over Antarctica, *J. Geophys. Res.*, 116, 1–16, doi:10.1029/2011JD015828, 2011.

Comparison of aeolian snow transport events and snow mass fluxes

A. Trouvilliez et al.

Title Page

Abstract

Introduction

Conclusions

References

Tables

Figures



Back

Close

Full Screen / Esc

Printer-friendly Version

Interactive Discussion



- Parish, T. R. and Wendler, G.: The katabatic wind regime at Adélie Land, Antarctica, *Int. J. Climatol.*, 11, 97–107, 1991.
- Pomeroy, J. W.: A process-based model of snow drifting, *J. Glaciol.*, 13, 237–240, 1989.
- Pomeroy, J. W. and Male, D. H.: Steady-state suspension of snow, *J. Hydrol.*, 136, 275–301, doi:10.1016/0022-1694(92)90015-N, 1992.
- Prud'homme, A. and Valtat, B.: Les observations météorologiques en Terre Adélie 1950–1952 – Analyse critique, *Expéditions polaires françaises*, Paris, 1957.
- Radok, U.: Snow Drift, *J. Glaciol.*, 19, 123–139, 1977.
- Scarchilli, C., Frezzotti, M., Grigioni, P., De Silvestri, L., Agnoletto, L., and Dolci, S.: Extraordinary blowing snow transport events in East Antarctica, *Clim. Dynam.*, 34, 1195–1206, doi:10.1007/s00382-009-0601-0, 2010.
- Sørensen, M.: An analytic model of wind-blown sand transport, in *Acta Mechanica (Suppl.)*, Vol. 1, edited by: Barndorff-Nielsen, O. and Willetts, B., 1–19, Springer, Vienna, 1991.
- Trouvilliez, A., Naaïm-Bouvet, F., Genthon, C., Luc, P., Favier, V., Bellot, H., Agosta, C., Palerme, C., Amory, C., and Gallée, H.: A novel experimental study of aeolian snow transport in Adélie Land (Antarctica), *Cold Reg. Sci. Technol.*, 108, 125–138, doi:10.1016/j.coldregions.2014.09.005, 2014.
- Trouvilliez, A., Naaïm-Bouvet, F., Bellot, H., Genthon, C., and Gallée, H.: Evaluation of Flowcap acoustic sensor for snowdrift measurements, *J. Atmos. Ocean. Tech.*, submitted, 2014.
- Wamser, C. and Lykossov, V. N.: On the friction velocity during blowing snow, *Contrib. to Atmos. Phys.*, 68, 85–94, 1995.
- Wendler, G.: On the blowing snow in Adélie Land, eastern Antarctica. A contribution to I. A. G.O. in: *Glacier fluctuations and climatic change*, edited by: Oerlemans, J., 261–279, Kluwer Academic Publishers, Reidel, Dordrecht, 1989.
- Wendler, G., Stearns, C. R., Dargaud, G., and Parish, T. R.: On the extraordinary katabatic winds of Adélie Land, *J. Geophys. Res.*, 102, 4463–4474, 1997.
- Wilkinson, R. H.: A Method for Evaluating Statistical Errors Associated with Logarithmic Velocity Profiles, *Geo.-Mar. Lett.*, 3, 49–52, 1984.
- Xiao, J., Bintanja, R., Déry, S. J., Mann, G. W., and Taylor, P. A.: An intercomparison among four models of blowing snow, *Bound.-Lay. Meteorol.*, 97, 109–135, 2000.

Comparison of aeolian snow transport events and snow mass fluxes

A. Trouvilliez et al.

Title Page

Abstract

Introduction

Conclusions

References

Tables

Figures

◀

▶

◀

▶

Back

Close

Full Screen / Esc

Printer-friendly Version

Interactive Discussion



Table 1. Localisation and description of the automatic weather and snow stations installed in Adélie Land.

	D3	D17	D47
Localisation	66.694 S, 139.898 E, 110 m a.s.l.	66.724 S, 139.706 E, 465 m a.s.l.	67.393 S, 138.709 E, 1565 m a.s.l.
Since	Feb 2009	Feb 2010	Jan 2010
Atmospheric measure- ments	Wind speed, tempera- ture and hygrometry at 2 m	Wind speed, tempera- ture and hygrometry at 6 levels	Wind speed, tempera- ture and hygrometry at 2 m
Blowing snow mea- surements	First generation FlowCapt™ from 0 to 1, 1 to 2 and 2 to 3 m	Second generation FlowCapt™ from 0 to 1 m	Second generation FlowCapt™ from 0 to 1 and 1 to 2 m

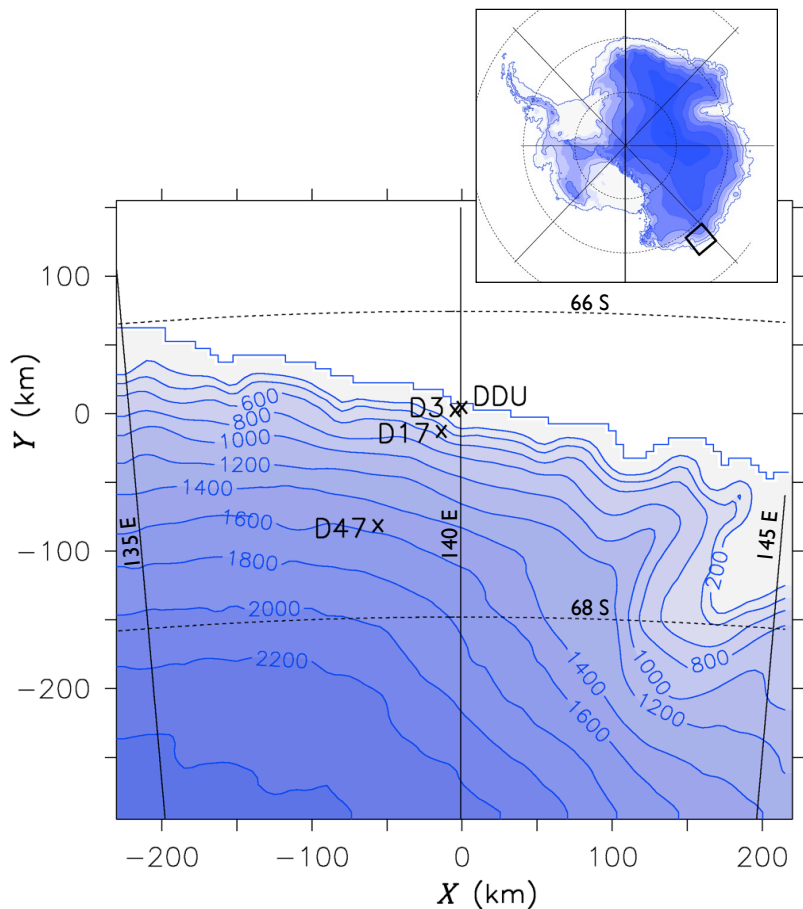


Figure 1. Integrative domain of the MAR in Adélie Land, East Antarctica. Crosses represent the Dumont D’Urville station (DDU), two automatic weather and snow stations used in this study (D17 and D47) and D3, which was the former station used in Gallée et al. (2013).

**Comparison of
aeolian snow
transport events and
snow mass fluxes**

A. Trouvilliez et al.

Title Page	
Abstract	Introduction
Conclusions	References
Tables	Figures
◀	▶
◀	▶
Back	Close
Full Screen / Esc	
Printer-friendly Version	
Interactive Discussion	





Figure 2. Left: the D17 7 m mast with one second-generation FlowCapt™ and Right: the D47 automatic weather and snow station with two second-generation FlowCapt™ sensors.

TCD

8, 6007–6032, 2014

Comparison of aeolian snow transport events and snow mass fluxes

A. Trouvilliez et al.

Title Page

Abstract

Introduction

Conclusions

References

Tables

Figures

◀

▶

◀

▶

Back

Close

Full Screen / Esc

Printer-friendly Version

Interactive Discussion



Comparison of aeolian snow transport events and snow mass fluxes

A. Trouvilliez et al.

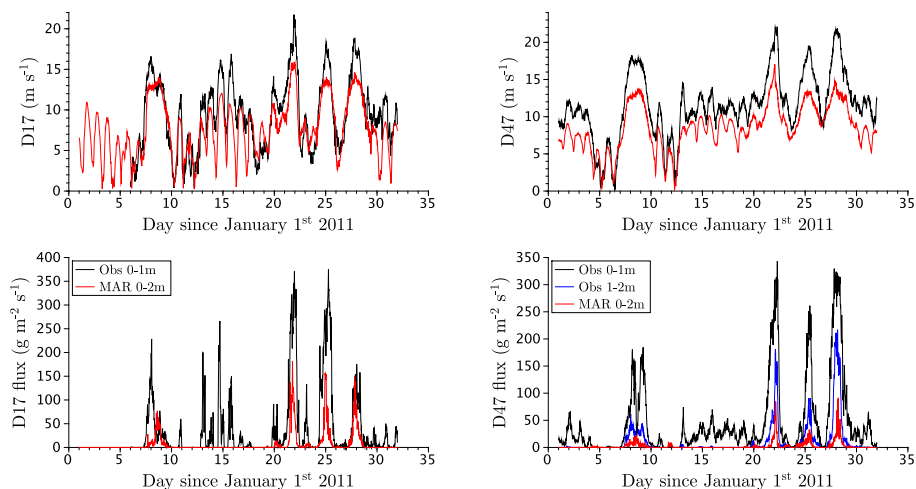


Figure 3. Top: observed (black) and simulated (red) wind speed at 2 m height. Bottom: aeolian snow transport events comparison between observed snow mass fluxes from 0 to 1 m (black) and simulated ones from 0 to 2 m (red) for the D17 site (bottom left) and the D47 site (bottom right). The observed snow mass fluxes from 1 to 2 m (blue) are also represented for the D47 site.

Comparison of aeolian snow transport events and snow mass fluxes

A. Trouvilliez et al.

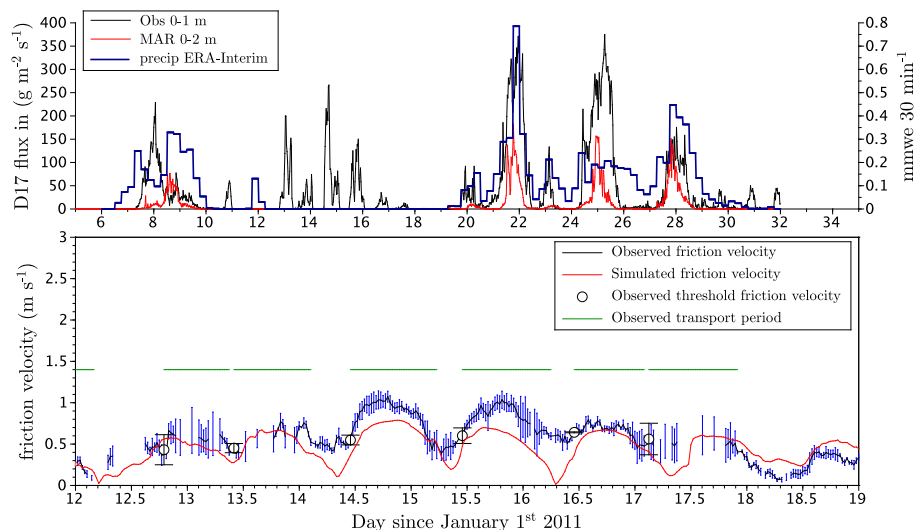


Figure 4. Top: comparison of aeolian snow transport events between observed snow mass fluxes from 0 to 1 m (black), simulated ones from 0 to 2 m (red) and precipitation from ERA-interim for the D17 site. Bottom: observed friction velocity (black line) at D17 and observed threshold friction velocity (black dot). The blue bars represent the 95% confidence limit of the friction velocity. The horizontal green bar represents the observed aeolian snow transport periods numbered from 1 to 6.

Title Page

Abstract

Introduction

Conclusions

References

Tables

Figures

◀

▶

◀

▶

Back

Close

Full Screen / Esc

Printer-friendly Version

Interactive Discussion

Comparison of aeolian snow transport events and snow mass fluxes

A. Trouvilliez et al.

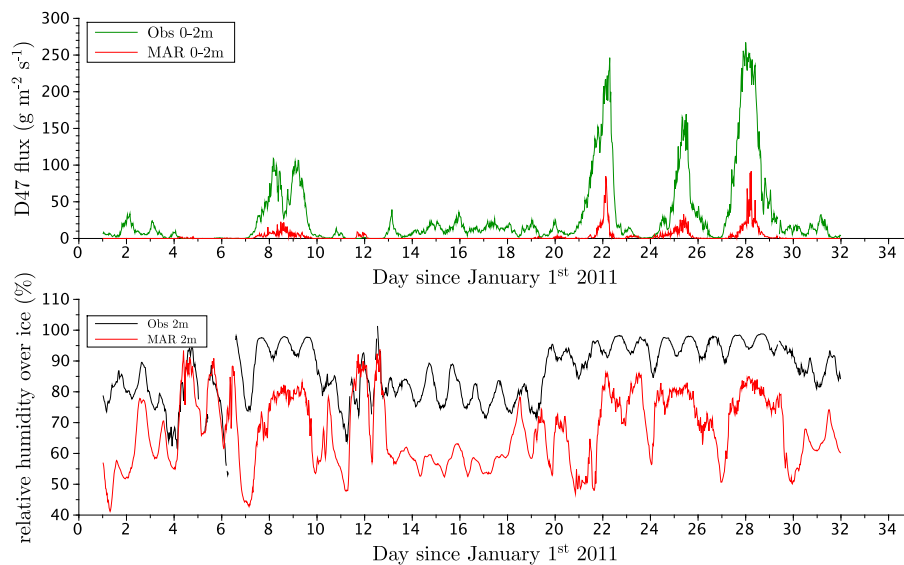


Figure 5. Top: observed (green) and simulated (red) snow mass fluxes from 0 to 2 m. Bottom: observed (black) and simulated (red) relative humidity over ice at 2 m.

[Title Page](#)[Abstract](#)[Introduction](#)[Conclusions](#)[References](#)[Tables](#)[Figures](#)[◀](#)[▶](#)[◀](#)[▶](#)[Back](#)[Close](#)[Full Screen / Esc](#)[Printer-friendly Version](#)[Interactive Discussion](#)

Comparison of aeolian snow transport events and snow mass fluxes

A. Trouvilliez et al.

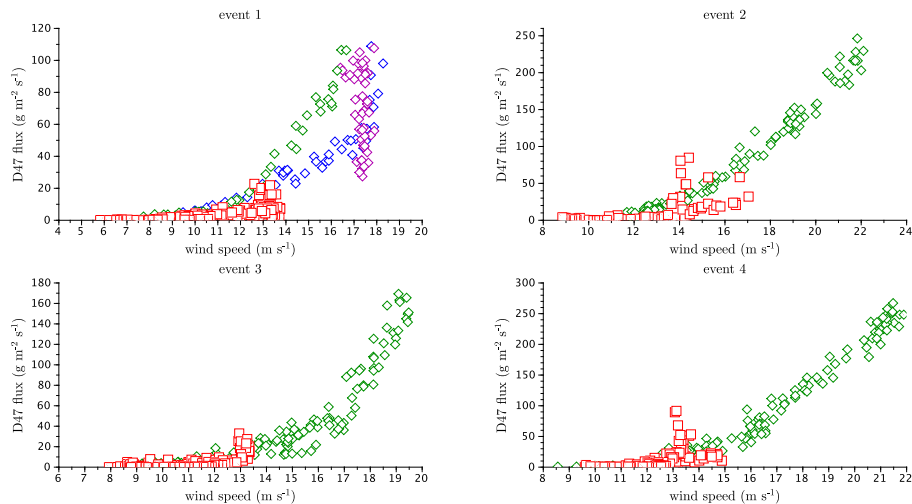


Figure 6. Observed (diamond) and simulated (red square) snow mass fluxes vs. the observed (and simulated respectively) wind speed in January 2011 from 0 to 2 m for the four strong aeolian snow transport events. Event 1 is from the 7th to the 10th, event 2 from the 21th to the 22th, event 3 from the 24th to the 26th and event 4 from the 27th to the 29th. For the first event, the observed snow mass fluxes are decomposed in time between a first (blue), an intermediate (purple) and a final relationship (green).

[Title Page](#)[Abstract](#)[Introduction](#)[Conclusions](#)[References](#)[Tables](#)[Figures](#)[Back](#)[Close](#)[Full Screen / Esc](#)[Printer-friendly Version](#)[Interactive Discussion](#)